



## Experimental and density functional theory study of the adsorption of N<sub>2</sub>O on ion-exchanged ZSM-5: Part II. The adsorption of N<sub>2</sub>O on main-group ion-exchanged ZSM-5

Bo Zhang<sup>1</sup>, Yongan Lu<sup>2</sup>, Hong He<sup>1,\*</sup>, Jianguo Wang<sup>2,\*</sup>, Changbin Zhang<sup>1</sup>, Yunbo Yu<sup>1</sup>, Li Xue<sup>1</sup>

1. Research Center for Eco-Environmental Sciences, Chinese Academy of Sciences, Beijing 100085, China. E-mail: [bozhang@rcees.ac.cn](mailto:bozhang@rcees.ac.cn)

2. College of Chemical Engineering and Materials Science, Zhejiang University of Technology, Hangzhou 310032, China

Received 24 May 2010; revised 16 August 2010; accepted 12 October 2010

### Abstract

The adsorption and desorption of N<sub>2</sub>O on main-group ion-exchanged ZSM-5 was studied using temperature-programmed desorption (TPD) and density functional theory (DFT) calculations. TPD experiments were carried out to determine the desorbed temperature  $T_{\max}$  corresponding to the maximum mass intensity of N<sub>2</sub>O desorption peak and adsorption capacity of N<sub>2</sub>O on metal-ion-exchanged ZSM-5s. The results indicated that  $T_{\max}$  followed a sequence of  $\text{Ba}^{2+} > \text{Ca}^{2+} > \text{Cs}^+ > \text{K}^+ > \text{Na}^+ > \text{Mg}^{2+}$  and the amount of adsorbed N<sub>2</sub>O on main-group metal cation followed a sequence of  $\text{Ba}^{2+} > \text{Mg}^{2+} > \text{Ca}^{2+} > \text{Na}^+ > \text{K}^+ > \text{Cs}^+$ . The DFT calculations were performed to obtain the adsorption energy ( $E_{\text{ads}}$ ), which represents the strength of the interaction between metal cations and the N-end or O-end of N<sub>2</sub>O. The calculation results showed that the N-end of the N<sub>2</sub>O molecule was favorably adsorbed on ion-exchanged ZSM-5, except for Cs-ZSM-5. For alkali metal cations, the  $E_{\text{ads}}$  of N<sub>2</sub>O on cations followed the order which was the same to that of  $T_{\max}$ :  $\text{Cs}^+ > \text{K}^+ > \text{Na}^+$ . The calculated and experimental results consistently showed that the adsorption performances of alkaline-earth metal cations were better than those of alkali metal cations.

**Key words:** N<sub>2</sub>O adsorption; ZSM-5; DFT; ion-exchanged zeolites

**DOI:** 10.1016/S1001-0742(10)60482-2

**Citation:** Zhang B, Lu Y G, He H, Wang J G, Zhang C B, Yu Y B et al., 2011. Experimental and density functional theory study of the adsorption of N<sub>2</sub>O on ion-exchanged ZSM-5: Part II. The adsorption of N<sub>2</sub>O on main-group ion-exchanged ZSM-5. Journal of Environmental Sciences, 23(4): 681–686

### Introduction

Nitrous oxide (N<sub>2</sub>O) is a greenhouse gas that has been proved to contribute to ozone destruction in the stratosphere (Ravishankara et al., 2009; Stott et al., 2002). Although N<sub>2</sub>O is not the major contributor to global warming (ca. 6%), its effects are much more potent than those of CO<sub>2</sub> and CH<sub>4</sub>. In addition, the destructive effects of N<sub>2</sub>O are compounded by the fact that N<sub>2</sub>O is a major stratospheric source of NO<sub>x</sub>. Anthropogenic practices, have led to a rapid increase in atmospheric N<sub>2</sub>O concentrations, with an annual growth rate of 0.2%–0.3% (Stott et al., 2002). Therefore, the control of N<sub>2</sub>O emissions from stationary and mobile combustion processes and from chemical processes has become a significant concern.

For decades, the catalytic decomposition of N<sub>2</sub>O to N<sub>2</sub> and O<sub>2</sub> has been widely investigated on transition-metals ion-exchanged zeolites (Pirngruber et al., 2006; Li and Armor, 1992; Waclaw et al., 2004). N<sub>2</sub>O adsorption on zeolites was observed in the catalytic decomposition of N<sub>2</sub>O

and in the reduction of N<sub>2</sub>O by hydrocarbons (Kapteijn et al., 1996; Pérez-Ramírez et al., 2003; Xue et al., 2007a, 2007b). Since N<sub>2</sub>O adsorption can be performed at room temperature and does not consume any additional energy, it can be regarded as an economic and environment-friendly method for N<sub>2</sub>O removal, particularly at low temperatures and/or at low emitted concentrations of the gas. Centi et al. (2000) studied the N<sub>2</sub>O adsorption on various ion-exchanged ZSM-5, X and Y zeolites. They concluded that Ba-ZSM-5 has a better adsorption capacity for N<sub>2</sub>O than other zeolites even in the presence of larger amounts of water. To develop new materials for N<sub>2</sub>O adsorption, the rules of adsorption for N<sub>2</sub>O on ion-exchanged zeolites require further research.

The calculations of the N<sub>2</sub>O adsorption were mainly focused on the transition-metal and noble metal cations, such as copper-, iron-, cobalt-, silver- gold- palladium-exchanged ZSM-5 (Kapteijn et al., 1996; Rakic et al., 2005; Zhanpeisov et al., 2003; Kameoka et al., 2001; Ates and Reitzmann, 2005a, 2005b; Lzumi et al., 2001; Yahiro and Iwamoto, 2001). Only one study on the adsorption of N<sub>2</sub>O over main-group ion-exchanged zeolites

\* Corresponding author. E-mail: [honghe@rcees.ac.cn](mailto:honghe@rcees.ac.cn) (Hong He); [jgw@zjut.edu.cn](mailto:jgw@zjut.edu.cn) (Jianguo Wang)

[www.jesc.ac.cn](http://www.jesc.ac.cn)

was published (Solkan et al., 2007). In this study, the activation energies for N<sub>2</sub>O dissociation on Ga-ZSM-5 and GaO-ZSM-5 at the B3LYP/6-31+G\* level (Becke's three-parameter hybrid method with the Lee, Yang and Parr gradient-corrected correlation functional, 6-31+G(d) basis set) were calculated by two full 10-membered zeolite rings model, and the possible reaction pathway for the catalytic dissociation of N<sub>2</sub>O was proposed. Lund (2006) used two models including 5T cluster model and two full 10-membered zeolite rings to calculate the minimum energy structures of surface intermediates on Fe/ZSM-5 catalyst. The results demonstrated that the 5T cluster is sufficiently accurate for calculating energies of structure, while the two full 10-membered zeolite rings are preferred for calculating the accurate geometries of the sites. Additionally, they concluded that the longer-range interactions between surface species and the ZSM-5 zeolite channel wall do not significantly affect the energies of the mechanistic steps. Moreover, previous studies (Heyden et al., 2005a, 2005b, 2006; Ryder et al., 2002) used 5T cluster model and the first principles to simulate the reaction mechanism of N<sub>2</sub>O dissociation over Fe-ZSM-5. They proved that the calculation can provide a satisfactory basis for simulating all of the experimental works. Therefore, 5T cluster model is suitable to calculate the adsorption energy of N<sub>2</sub>O on metal ion-exchanged ZSM-5.

In this article, the experimental results of temperature-programmed desorption (TPD) were compared with the predictions made by density functional theory (DFT) calculations in an analysis of the adsorption behavior of N<sub>2</sub>O on ZSM-5 zeolites exchanged with six main group metal cations (Na<sup>+</sup>, K<sup>+</sup>, Cs<sup>+</sup>, Mg<sup>2+</sup>, Ca<sup>2+</sup>, and Ba<sup>2+</sup>). The aim of the research was to determine the rules governing the N<sub>2</sub>O adsorption potential on main-group ion-exchanged ZSM-5 with respect to the influence of ionic radius, electrostatic field.

## 1 Experimental methods

### 1.1 Materials preparation and characterization

All samples were prepared by the wet ion-exchange method. Typically, 10 g H-ZSM-5 (SiO<sub>2</sub>/Al<sub>2</sub>O<sub>3</sub> = 25, Nankai University, China) was mixed with 80 mL of 0.2 mol/L nitrate salts solution at 90°C for 24 hr. After ion exchange, the samples were filtered, thoroughly washed, dried overnight at 100°C, and then calcined in air at 550°C for 4 hr to obtain cation-exchanged-ZSM-5. Several alkali and alkali earth cations were selected including Na<sup>+</sup>, K<sup>+</sup>, Cs<sup>+</sup>, Mg<sup>2+</sup>, Ca<sup>2+</sup>, and Ba<sup>2+</sup>.

The Si, Al, and metal ions contents of these zeolites were determined by inductively coupled plasma optical emission spectrometer (ICP-OES) using an Optima 2000 spectrometer (Perkin-Elmer Co., USA)

### 1.2 Desorption test

TPD test was performed on a Hiden analytical instrument, equipped with a quadrupole mass spectrometry (QMS) sampling system (HPR20, Hiden Analytical Ltd.,

UK). Briefly, 1.0 g zeolites (mesh size: 0.5–0.25 mm) was placed in the tubular quartz reactor. The 0.5-mm (OD) thermocouples measured the temperature of the adsorbent bed and provided feedback to the temperature programmer. Prior to N<sub>2</sub>O adsorption in 2% N<sub>2</sub>O/Ar at room temperature, all zeolites were pretreated in a flow of 20% O<sub>2</sub>/Ar at 500°C for 1 hr. After the zeolites were saturated with N<sub>2</sub>O, the physical desorption of N<sub>2</sub>O was performed using Ar for 1 hr at room temperature. Subsequently, the temperature was raised by 30°C/min from room temperature to 500°C. The signals of N<sub>2</sub>O (*m/z* = 44) and NO (*m/z* = 30) were collected simultaneously by mass spectrometry.

## 2 Model development and calculation

In this study, the 5T cluster model is identical to that used in previous publications (Heyden et al., 2005a, 2005b, 2006; Ryder et al., 2002). The portion of the cluster describing the zeolite contains an Al-atom in the T12 position of the framework surrounded by shells of O- and Si-atoms. The terminal Si-atoms are fixed in their crystallographic positions, as reported by Olson et al. (1981). Dangling bonds are terminated by H-atoms.

The first-principles DFT calculations were carried out using the DMol3 package (Delley et al., 1990, 2000). The generalized gradient approximation (GGA) with PW91 functional (Perdew and Wang, 1992) was used to describe the exchange-correlation (XC) effects. The double numerical with polarization functions (DNP) basis set was used in the expanded electronic wave functional. Therefore, all of calculations were performed by using spin-restricted methods by choosing suitable spin multiplicity for different cations. The convergence criterions in energy and force were set to 10<sup>-5</sup> eV and 2 × 10<sup>-3</sup> eV/Å, respectively.

The adsorption potential energies were calculated according to the following equation:

$$E_{\text{ads}} = E_{\text{complex}} (E_{\text{ZSM-5}} + E_{\text{adsorbate}})$$

where,  $E_{\text{ads}}$  is the adsorption energy;  $E_{\text{complex}}$  is the total energy of the ZSM-5 with the adsorbate; and  $E_{\text{adsorbate}}$  and  $E_{\text{ZSM-5}}$  are the energies of isolated adsorbate and ZSM-5, respectively.

## 3 Results and discussion

### 3.1 Desorption test

N<sub>2</sub>O-TPD experiments were carried out to study the adsorption and desorption behaviors of N<sub>2</sub>O on main-group metal ion-exchanged ZSM-5s. The desorbed temperature  $T_{\text{max}}$  corresponding to the maximum mass intensity of N<sub>2</sub>O desorption peak was used to evaluate the strength of N<sub>2</sub>O adsorption onto cations. The amount of adsorbed N<sub>2</sub>O was calculated from TPD profiles to estimate the adsorption capacity of the various zeolites.

Figure 1 illustrates that desorption of N<sub>2</sub>O occurred at temperatures below 200°C on all of the ion-exchanged ZSM-5 zeolites. For HZSM-5, only trace amounts of N<sub>2</sub>O desorbed in the TPD experiment. The dramatic increase in

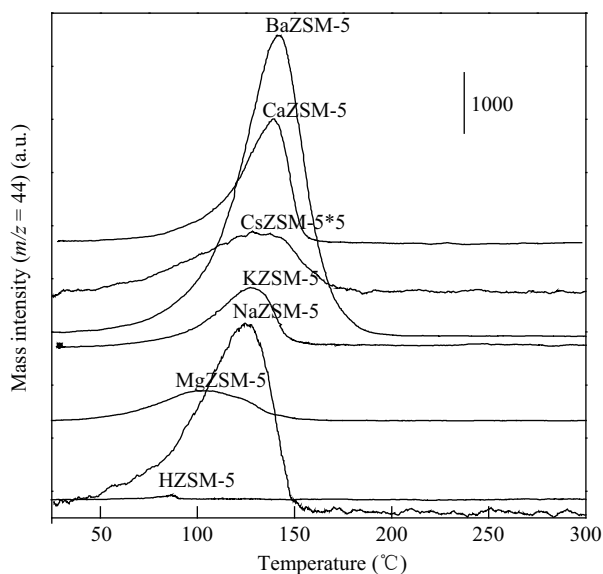


**Fig. 1** Temperature-programmed desorption of N<sub>2</sub>O on main-group metal ion-exchanged ZSM-5.

the adsorption of N<sub>2</sub>O on ion-exchanged ZSM-5 indicates that metal cations play a crucial role in N<sub>2</sub>O adsorption. There was only one desorption peak in each TPD profile and areas of these peaks were quite different from each other. Thus, it is concluded that the nature of the metal cation in ZSM-5 significantly influenced the adsorption behavior.  $T_{\max}$  and amounts of adsorbed gases obtained from TPD profiles are summarized in Table 1.

As shown in Table 1,  $T_{\max}$  and the amount of adsorbed N<sub>2</sub>O on per main group metal cations followed the order of  $\text{Ba}^{2+} > \text{Ca}^{2+} > \text{Cs}^+ > \text{K}^+ > \text{Na}^+ > \text{Mg}^{2+}$  and  $\text{Ba}^{2+} > \text{Mg}^{2+} > \text{Ca}^{2+} > \text{Cs}^+ > \text{Na}^+ > \text{K}^+$ , respectively. These results indicate that the adsorption performances of alkaline-earth metal cations were better than those of alkali metal cations. Ba-ZSM-5 exhibited the best adsorption behavior, including the highest desorption temperature and adsorption capacity, which is consistent with published work (Centi et al., 2000). For N<sub>2</sub>O adsorption capacity of zeolites, the amount of adsorbed N<sub>2</sub>O is  $10^{-6}$  mol N<sub>2</sub>O/g zeolite which is less than the value of  $6 \times 10^{-5}$ – $14.9 \times 10^{-5}$  mol N<sub>2</sub>O/g zeolite reported by Groen et al. (2002). In our study, the pretreatment of zeolites and the adsorption of N<sub>2</sub>O were performed in the flow of 2% N<sub>2</sub>O/Ar in ambient pressure. In contrast, experiments were performed *in situ* vacuum

**Table 1** Adsorption of N<sub>2</sub>O on various ion-exchanged ZSM-5 samples at room temperature

Me-ZSM-5	$T_{\max}$ (°C)	Exchange level <sup>a</sup> (%)	Absorption amount <sup>b</sup> ( $10^{-6}$ mol N <sub>2</sub> O/ g zeolite)	Molar ratio of N <sub>2</sub> O/Me <sup>c</sup> $\times 10^{-2}$
Mg <sup>2+</sup>	102	14.9	9.1	7.8
Na <sup>+</sup>	125	100	15.2	2.2
K <sup>+</sup>	129	100	11.35	1.47
Cs <sup>+</sup>	135	10	0.21	2.4
Ca <sup>2+</sup>	136	22.5	11.8	5.72
Ba <sup>2+</sup>	140	41.2	250.3	94.9

<sup>a</sup> The exchange level is estimated on the basis of the  $\text{Me}^{n+}/\text{Al}$  molar ratio; <sup>b</sup> the maximum adsorbed moles of N<sub>2</sub>O on per gram of zeolite are estimated from the area of TPD peak; <sup>c</sup> the mole ratio of N<sub>2</sub>O and cations reflect the amount of adsorbed N<sub>2</sub>O on per 100 metal cations (Me).

system in the literature (Groen et al., 2002). Therefore, the great deference in these results suggests that the flow decrease the trapped N<sub>2</sub>O in the channel of zeolites.

The electrostatic field of the cation exchanged into the zeolite is important for the interaction between cation and adsorbate (Blatter and Frei, 1993, 1994). As mentioned in literature, if main-group cations were exchanged into the zeolites, a strong electrostatic field could highly polarize the N<sub>2</sub>O molecule into the  $\text{N} = \text{N}^+ - \text{O}^-$  resonance form which may be favorable for stabilizing the N<sub>2</sub>O molecule in zeolite channels (Centi et al., 2000). Cations with small radii interact strongly with N<sub>2</sub>O at a short distance. On this basis, the  $T_{\max}$  of Mg<sup>2+</sup>, which has a small radius of 72 pm, should be the highest. However, the  $T_{\max}$  of Mg<sup>2+</sup> at 102°C is the lowest among all of the studied cations. It can be considered that the large ionic radius can increase the effective action area between the cation and N<sub>2</sub>O, which is positively related to the strength of their interaction. Accordingly, Ba<sup>2+</sup> and Cs<sup>+</sup>, with the largest radii in their group, exhibited the best strength of adsorption. For Mg<sup>2+</sup>-exchanged zeolites, the very small effective action area between Mg<sup>2+</sup> and N<sub>2</sub>O molecule probably weakened their interaction, thereby inducing the lowest  $T_{\max}$ . Therefore, to the same main group cations, large radii can promote the interaction between cation and N<sub>2</sub>O.

### 3.2 Calculations

In order to rationalize the experimental results, DFT calculations were performed to investigate the adsorption energy, geometric and electronic properties of N<sub>2</sub>O on various main-group metal ion exchange ZSM-5 zeolite.

Figure 2 shows the optimized configuration of the N<sub>2</sub>O molecule adsorbed on Mg-ZSM-5, with the N-end (Fig. 2a) and the O-end (Fig. 2b). Similar configurations were adopted for the other ion-exchanged ZSM-5s. The bond lengths of N–N and N–O in N<sub>2</sub>O as well as the adsorption energies of N<sub>2</sub>O adsorbed on ion-exchanged ZSM-5s were calculated based on the above models. As presented in Table 2, geometrical and energetic changes took place during the adsorption process of N<sub>2</sub>O on metal-ion-exchanged ZSM-5. For example, the calculated values of the N–N and N–O bond lengths in the free N<sub>2</sub>O molecule are 1.12 and 1.18 Å, respectively. When N<sub>2</sub>O is adsorbed onto various ion-exchanged ZSM-5s through its

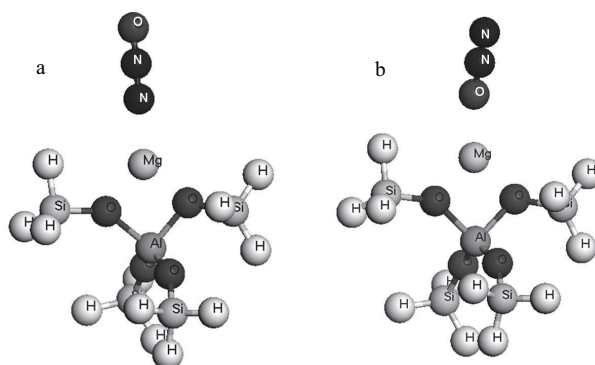


**Fig. 2** Optimized configuration of N<sub>2</sub>O molecule adsorbed on Mg-ZSM-5 through N-end (a) or O-end (b).

N-end, the N–N bonds elongate, according to the calculation results. The adsorption energies of N<sub>2</sub>O molecules on several ion-exchanged ZSM-5s are compared in Fig. 3.

From the data provided in Table 2 and Fig. 3, it is apparent that the N-end is more favorable for N<sub>2</sub>O adsorption on various ion-exchanged ZSM-5s, except for Cs<sup>+</sup>-ZSM-5. For most of ion-exchanged ZSM-5, adsorption of the N-end of N<sub>2</sub>O and NO was favored, consistent with the results of previous calculations (Ghosh et al., 2003; Rakic et al., 2005; Yajima et al., 2000; Zhanpeisov et al., 2003; Miyamoto, 2000). There was no corresponding work on the adsorption of N<sub>2</sub>O on Cs<sup>+</sup>-ZSM-5. We analyzed N-end adsorption, as presented and discussed in the following sections. According to the  $E_{\text{ads}}$  (N-end N<sub>2</sub>O) value, the adsorption strength of N<sub>2</sub>O on the main-group ions followed the order: Mg<sup>2+</sup> > Ca<sup>2+</sup> > Cs<sup>+</sup> > K<sup>+</sup> > Ba<sup>2+</sup> > Na<sup>+</sup>.

Compared with the  $T_{\text{max}}$  order, Ba<sup>2+</sup> > Ca<sup>2+</sup> > Cs<sup>+</sup> > K<sup>+</sup> > Na<sup>+</sup> > Mg<sup>2+</sup>, it is found that the adsorption strength

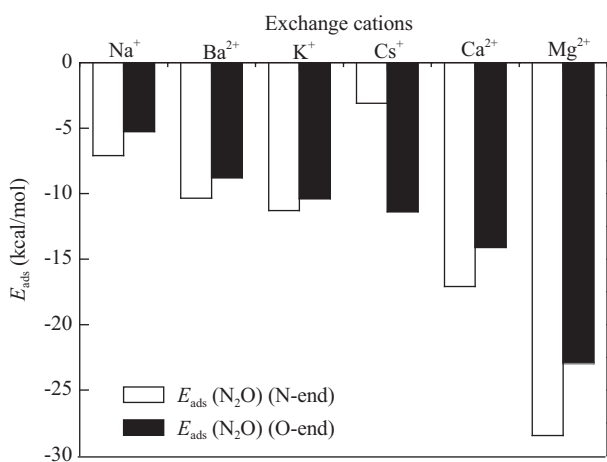


**Fig. 3** Adsorption energies of N<sub>2</sub>O on various ion-exchanged ZSM-5s (N-end and O-end).

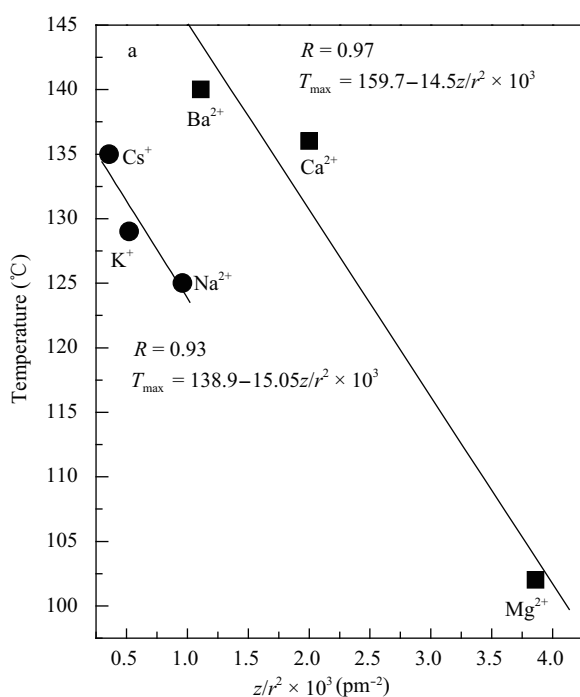


**Table 2** Adsorption energies of N<sub>2</sub>O on various ion-exchanged ZSM-5s and bond length of N–N and N–O in N<sub>2</sub>O molecule adsorbed on zeolites with O-end

Metal ion (ionic radius (pm)) <sup>a</sup>	$E_{\text{ads}}$ (kcal/mol)		Bond length of N <sub>2</sub> O adsorbed with N-end (Å)	
	N-end	O-end	N–N (1.12 Å)	N–O (1.18 Å)
Mg <sup>2+</sup> (72)	28.46	22.97	1.14	1.16
K <sup>+</sup> (138)	11.33	10.38	1.14	1.19
Na <sup>+</sup> (102)	7.1	5.26	1.14	1.18
Cs <sup>+</sup> (167)	3.1	11.37	1.14	1.12
Ba <sup>2+</sup> (135)	10.35	8.77	1.21	1.18
Ca <sup>2+</sup> (100)	17.08	14.11	1.14	1.17

<sup>a</sup> The ionic radius data quote from Wikipedia, the free encyclopedia.

between the alkali earth cations and N<sub>2</sub>O is basically higher than that of alkali cations. For the elements in the similar radius, i.e., Na<sup>+</sup> (102 pm) and Ca<sup>2+</sup> (100 pm), K<sup>+</sup> (138 pm) and Ba<sup>2+</sup> (135 pm), the valence of cations is important to the association between N<sub>2</sub>O and cations.

According to experimental and calculation results, the electrostatic force of cations  $F = k \frac{z}{r^2}$  ( $z$  is charge and  $r$  is radius of cation) was considered to be responsible to the rules of  $T_{\text{max}}$  and  $E_{\text{ads}}$ . The relationship between  $T_{\text{max}}$ ,  $E_{\text{ads}}$  and electrostatic force is shown in Fig. 4. For the elements in the same group,  $T_{\text{max}}$  is inversely related with the electrostatic force between cations and N<sub>2</sub>O molecular (Fig. 4a). It indicates that the cation radius plays a key role in the association between N<sub>2</sub>O and main-group cations. Accordingly, Ba<sup>2+</sup> and Cs<sup>+</sup>, with the largest radii in their group, exhibited the best strength of adsorption. In Fig. 4b, for alkali earth cations, the  $E_{\text{ads}}$  value is proportional to  $F$ , while the converse occurred in alkali cations. For alkali cations, the  $E_{\text{ads}}$  of N<sub>2</sub>O on the cations follows the order which is absolutely same to that of the  $T_{\text{max}}$ : Cs<sup>+</sup> > K<sup>+</sup> > Na<sup>+</sup>. However, to alkali earth cations, the order of  $T_{\text{max}}$  converses to that of  $E_{\text{ads}}$ , suggesting that the

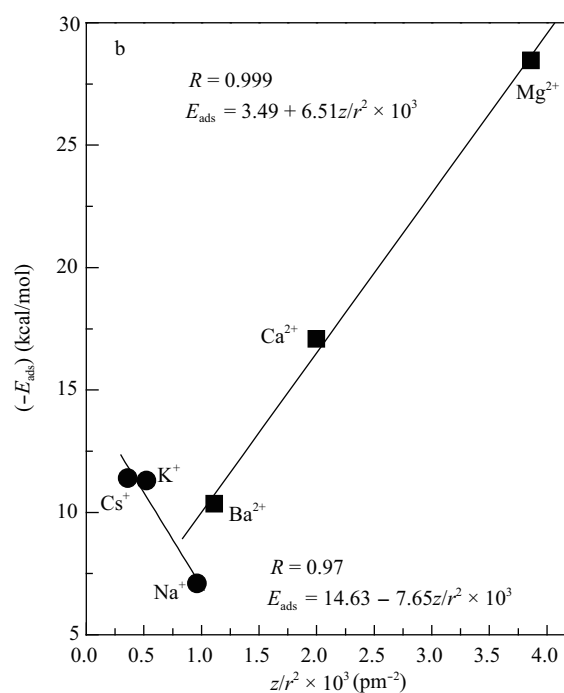


**Fig. 4** Relationship between  $T_{\text{max}}$  (a) and  $E_{\text{ads}}$  (b) with electrostatic force.

current calculated method is probably unsuitable to study the adsorption behavior of gas molecular, or other factor need to be considered. The research of the calculation on the adsorption of N<sub>2</sub>O over alkali earth cations will be developed.

On the basis of the above analysis of the data, it is found that the radius has two conflicting aspects influencing the adsorption strength of cations. On one hand, a small radius can increase the Coulombic force between main-group-metal cations and N<sub>2</sub>O. On the other hand, a large radius can increase the effective action area of these cations and N<sub>2</sub>O promoting the association between cations and N<sub>2</sub>O. Experimental results undoubtedly prove that the effective action area of the cations is the main determinant of adsorption strength.

## 4 Conclusions

Experimental results showed that high valence and a large radius favor the strong interaction of main-group-metal cations with N<sub>2</sub>O, Ba-ZSM-5 exhibited the best adsorption behavior, including the highest desorption temperature and adsorption capacity. The DFT calculation results showed that the N-end of N<sub>2</sub>O is favorable in the molecule's adsorption on a set of ion-exchanged zeolites except in the cases of Cs-ZSM-5. The behavior of N<sub>2</sub>O adsorption on main-group-metals ion-exchanged ZSM-5 is influenced not only by the valence of these cations but also by their ionic radius. Theoretical and experimental results consistently indicated that the alkali earth cations were more favorable adsorption for N<sub>2</sub>O than alkali cations. For the alkali cations, the  $E_{\text{ads}}$  of N<sub>2</sub>O on cations follows the order which is absolutely same to that of the  $T_{\text{max}}$ : Cs<sup>+</sup> > K<sup>+</sup> > Na<sup>+</sup>. While the inverse rule of  $E_{\text{ads}}$  and  $T_{\text{max}}$  of alkali earth cations proved that the present calculation method is unsuitable to study the adsorption behavior of N<sub>2</sub>O on alkali earth metal ion-exchanged ZSM-5.

## Acknowledgments

This work was financially supported by the National Natural Science Foundation of China (No. 50921064, 20906081) and the National High Technology Research and Development Program (863) of China (No. 2007AA06Z314, 2009AA06Z301).

## References

- Ates A, Reitzmann A, 2005a. The interaction of N<sub>2</sub>O with ZSM-5-type zeolites: A transient, multipulse investigation. *Journal of Catalysis*, 235(1): 164–174.
- Ates A, Reitzmann A, 2005b. Transient multipulse method for the determination of N<sub>2</sub>O-interaction with ZSM-5 type zeolites. *Reaction Kinetics and Catalysis Letters*, 86(1): 11–20.
- Blatter F, Frei H, 1993. Very strong stabilization of alkene O<sub>2</sub> charge-transfer state in zeolite NaY: red-light-induced photooxidation of 2,3-dimethyl-2-butene. *Journal of American Chemical Society*, 115(16): 7501–7502.
- Blatter F, Frei H, 1994. Selective photooxidation of small alkenes by O<sub>2</sub> with red light in zeolite Y. *Journal of American Chemical Society*, 116(5): 1812–1820.
- Centi G, Generali P, dall'Olio L, Perathoner S, 2000. Removal of N<sub>2</sub>O from industrial gaseous streams by selective adsorption over metal-exchanged zeolites. *Industrial & Engineering Chemistry Research*, 39(1): 131–137.
- Delley B, 1990. An all-electron numerical-method for solving the local density functional for polyatomic-molecules. *Journal of Chemical Physics*, 92(1): 508–517.
- Delley B, 2000. From molecules to solids with the DMol(3) approach. *Journal of Chemical Physics*, 113(18): 7756–7764.
- Ghosh S, Gorelsky S I, Chen P, 2003. Activation of N<sub>2</sub>O reduction by the fully reduced  $\mu_4$ -sulfide bridged tetranuclear Cu<sub>4</sub> cluster in nitrous oxide reductase. *Journal of the American Chemical Society*, 125, 15708–15709.
- Groen J C, Pérez-Ramírez J, Zhu W, 2002. Adsorption of nitrous oxide on silicalite-1. *Journal of Chemical & Engineering Data*, 47(3): 587–589.
- Heyden A, Baron P, Bell A T, Keil F J, 2005a. Comprehensive DFT study of nitrous oxide decomposition over Fe-ZSM-5. *The Journal of Physical Chemistry B*, 109(5): 1857–1873.
- Heyden A, Bell A T, Keil F J, 2005b. Kinetic modeling of nitrous oxide decomposition on Fe-ZSM-5 based on parameters obtained from first-principles calculations. *Journal of Catalysis*, 233(1): 26–35.
- Heyden A, Hansen N, Bell A T, Keil F J, 2006. Nitrous oxide decomposition over Fe-ZSM-5 in the presence of nitric oxide: a comprehensive DFT study. *The Journal of Physical Chemistry B*, 110(34): 17096–17114.
- Kameoka S, Yuzaki K, Takeda T, Tanaka S I, Ito S I, Miyadera T et al., 2001. Selective catalytic reduction of N<sub>2</sub>O with C<sub>3</sub>H<sub>6</sub> over Fe-ZSM5 catalyst in the presence of excess O<sub>2</sub>: The correlation between the induction period and the surface species produced. *Physical Chemistry Chemical Physics*, 3(2): 256–260.
- Kapteijn F, Rodriguez-Mirasol J, Moulijn J A, 1996. Heterogeneous catalytic decomposition of nitrous oxide. *Applied Catalysis B*, 9: 25–64.
- Li Y, Armor J N, 1992. Catalytic decomposition of nitrous oxide on metal exchanged zeolites. *Applied Catalysis B*, 1(3): L21–L29.
- Lund C R F, 2006. Effects of zeolite channel walls and cation migration on N<sub>2</sub>O decomposition energies. *Journal of Catalysis*, 243(2): 438–441.
- Lzumi Y, Kizaki T, Aika K, 2001. Simultaneous removal of NO and N<sub>2</sub>O over Pd-ZSM-5 catalysts and FT-IR observations of their decomposition routes to N<sub>2</sub>. *Bulletin of the Chemical Society of Japan*, 74(8): 1499–1505.
- Miyamoto A, 2000. Combinatorial computational chemistry approach to the design of deNO<sub>x</sub> catalysts. *Applied Catalysis A*, 194: 183–191.
- Olson D H, Kokotalo G T, Law S L, Meler W M, 1981. Crystal structure and structure-related properties of ZSM-5. *Journal of Physical Chemistry*, 85(15): 2238–2243.
- Pérez-Ramírez J, Kapteijn F, 2003. Effect of NO on the catalytic removal of N<sub>2</sub>O over FeZSM-5. Friend or foe. *Catalysis Communication*, 4(7): 333–338.
- Pirngruber G D, Frunz L, Pieterse J A Z, 2006. The synergy between Fe and Ru in N<sub>2</sub>O decomposition over FeRu-FER catalysts: A mechanistic explanation. *Journal of Catalysis*, 243(2): 340–349.
- Rakic V, Rac V, Dondur V, Auroux A, 2005. Competitive adsorption of N<sub>2</sub>O and CO on CuZSM-5, FeZSM-5, CoZSM-5 and bimetallic forms of ZSM-5 zeolite. *Catalysis Today*, 110(3-4): 272–280.

- Ravishankara A R, Daniel J S, Portmann R W, 2009. Nitrous oxide ( $N_2O$ ): the dominant ozone-depleting substance emitted in the 21st century. *Science*, 326(5949): 123–125.
- Ryder J A, Chakraborty A K, Bell A T, 2002. Density functional theory study of nitrous oxide decomposition over Fe- and Co-ZSM-5. *Journal of the Physical Chemistry B*, 106(28): 7059–7064.
- Solkan V N, Zhidomirov G M, Kazansky V B, 2007. Density functional theory studies of nitrous oxide adsorption and decomposition on Ga-ZSM-5. *International Journal of Quantum Chemistry*, 107(13): 2417–2425.
- Stott L, Poulsen C, Lund S, Thunell R, 2002. Super ENSO and global climate oscillations at millennial time scales. *Science*, 297(5579): 222–226.
- Waclaw A, Nowinska K, Schwieger W, 2004.  $N_2O$  decomposition over iron modified zeolites ZSM-5. *Catalysis Today*, 90(1-2): 21–25.
- Xue L, Zhang C, He H, Teraoka Y, 2007a. Catalytic decomposition of  $N_2O$  over  $CeO_2$  promoted  $Co_3O_4$  spinel catalyst. *Applied Catalysis B*, 75(3-4): 167–174.
- Xue L, Zhang C, He H, Teraoka Y, 2007b. Promotion effect of residual K on the decomposition of  $N_2O$  over cobalt–cerium mixed oxide catalyst. *Catalysis Today*, 126(3-4): 449–455.
- Yahiro H, Iwamoto M, 2001. Copper ion-exchanged zeolite catalysts in deNO<sub>x</sub> reaction. *Applied Catalysis A*, 222(1-2): 163–181.
- Yajima K, Ueda Y, Tsuruya H, Kanougi T, Oumi Y, Salai S et al., 2000. Combinatorial computational chemistry approach to the design of deNO<sub>x</sub> catalysts. *Applied Catalysis A*, 194–195: 183–191.
- Zhanpeisov N U, Ju W S, Matsuoka M, Anpo M, 2003. Quantum chemical calculations on the structure and adsorption properties of NO and  $N_2O$  on  $Ag^+$  and  $Cu^+$  ion-exchanged zeolites. *Structure Chemistry*, 14(3): 247–255.